



Oil Spill Detection in Oceans using Threshold Segmentation and SVM classification

V. Vidya Lakshmi¹, Hemanth.G², Akshay Vignesh.R³, Ragul Barath. M.P⁴, Giridharan.P⁵
Assistant Professor¹, UG Student^{2, 3, 4, 5}

Department of Electronics and Communication Engineering
Velammal Engineering College, Chennai, Tamil Nadu, India

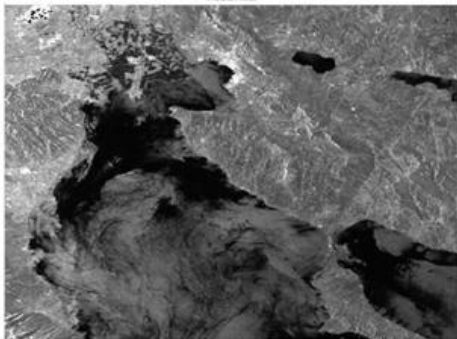
Abstract:

Oil spill is one of main environmental hazards in ocean pollution. Navigation radar as a basic device installed in vessels can be used for oil spill detection. This paper designs a characteristic attribute for marine oil-spilling accidents. Other methods are used for oil spills detection, such as optical sensor, synthetic aperture radar (SAR) and laser fluorosensor, marine navigation radar is a convenient, rapid and economical approach. In proposed method, oil spilling is detected by the segmentation (Thresholding), feature extraction process and classification (SVM). It is free from noise (median filter). In this system, we are detecting the exact oil spilling which does not involve any mathematical calculations.

Index Terms: Constant false alarm rate (CFAR), covariance matrix equality, invariance, multifamily generalized likelihood ratio test (MGLRT), oil spill detection, one-sided generalized likelihood ratio test (GLRT).

I. INTRODUCTION

OIL spills represent a threat to the environment, wildlife, and to human life through the food chain. Natural phenomena, oil pipeline breakages, and illegal human activities are the causes of the presence of oil spills in the sea. In particular, illegal washing activities of oil tankers contribute 70% to sea pollution with oil [1]. As this kind of activity is difficult to prevent, monitoring and detection of the phenomenon is vital to be able to act timely and avoid natural disasters. Oil spills have peculiar characteristics that make them visible in synthetic aperture radar (SAR) images. Oil smooths the sea surface, reducing its roughness, thus appearing darker in SAR images.



For this reason, at least in principle, SAR represents a powerful tool for oil spill detection and sizing [2]. Improved reliability in such detection process has been demonstrated, exploiting the additional information residing in the polarimetric returns. Recently, the topic of oil spill detection in polarimetric SAR has been investigated with different approaches. In [4], a feature extraction and maximum entropy segmentation approach has been proposed. The capabilities of hybrid/compact dual-polarization (dual-pol) modes have been

assessed in [5], with experimental results suggesting that hybrid/compact and (HH, VV) dual-pol modes deliver better detection performance compared with conventional dual-pol modes, i.e., (HH, HV) and (VH, VV). The potential of circular polarization coherence and polarimetric anisotropy has been assessed in [6], showing that the anisotropy is always higher within the slick area both in L- and C-bands. Decision schemes ensuring the constant false alarm rate (CFAR) property and the target decomposition theorem have been jointly used in [7] to detect and classify oil spills, highlighting that entropy plays a key role in the classification process. Three techniques based on the generalized likelihood ratio test (GLRT) and the maximum-likelihood estimate have been proposed in [8], providing near-optimal performance in real environment. Compact polarimetric (CP) mode has been proposed in [9] as an alternative transmission mode providing enhanced discriminating capabilities due to a specific X-Bragg scattering model. In [10], the CP mode has been also exploited; in particular, a quad-polarization representation of the data has been obtained from a circular transmit linear receive configuration and has been used for statistical detection of oil spills. Finally, future perspectives in oil slicks detection, including multisensor integration, have been suggested in [11].

II. EXISTING METHOD

In the existing method, the problem of oil spill detection is formulated in terms of a binary hypothesis test aimed at discriminating between the presence and the absence of variations in the polarimetric covariance matrix (PCM) of the radar returns. The idea is to compare the region under test, which possibly contains oil spills, to a reference area where only echoes from the sea are present. As already stated, the presence of oil damps short gravity-capillary waves down and

decreases the backscattering of sea surface. Thus, it is reasonable to assume that the PCM of data containing oil slicks shares eigenvalues smaller than or equal to the PCM of the sea returns. The decision problem is solved applying the GLRT, and the devised architecture is referred to as positive definite difference GLRT (PDD-GLRT). At the design stage, it is assumed that the rank difference between the two covariance matrices is known. However, this assumption might not be met in practical scenarios, since such *a priori* information is not available at the receiver. In order to circumvent this drawback, the previous results are extended to come up with a decision rule capable of properly estimating the rank difference. This goal is achieved exploiting the multifamily GLRT (MGLRT) [12], and the de-vised decision rule is referred to as the multifamily PDD-GLRT (M-PDD-GLRT). In addition, a discussion on the invariance properties of the PDD-GLRT (and, hence, of the M-PDD-GLRT) is provided. More precisely, the *invariance principle* is invoked to express the decision statistic in terms of a maximal invariant [13], [14]. Finally, numerical examples are provided to prove the effectiveness of the proposed approach also in comparison with existing strategies for oil spill detection. The remainder of this paper is organized as follows. Section II is devoted to the problem formulation. The derivations of the PDD-GLRT and its multifamily modification are reported in Section III, including details on the invariance and CFAR property. Section IV analyzes the performance in terms of detection probability on simulated and real data. Some concluding remarks and future research tracks are given in Section V. Finally, proofs and derivations are confined to the Appendixes. *Notation:* Vectors and matrices are denoted by boldface lowercase and uppercase letters, respectively. Symbols $\det(\cdot)$ and $\text{Tr}(\cdot)$ denote the determinant and the trace of a square matrix, respectively. Symbol \mathbb{H}^N is used to represent the set of $N \times N$ Hermitian matrices, whereas I and 0 represent the identity matrix and the null vector or matrix, respectively, both of suitable dimensions. The curled inequality symbol (and its strict form) is used to denote generalized matrix inequality: for any $A \in \mathbb{H}^N$, $A \succ 0$ means that A is a positive semidefinite matrix ($A \succ 0$ for positive definiteness). As to the numerical sets, \mathbb{R} is the set of real numbers, $\mathbb{R}^{N \times M}$ is the set of $(N \times M)$ -dimensional real matrices (or vectors if $M = 1$), \mathbb{C} is the set of complex numbers, and $\mathbb{C}^{N \times M}$ is the set of $(N \times M)$ -dimensional complex matrices (or vectors if $M = 1$). Symbols $(\cdot)^T$ and $(\cdot)^*$ stand for transpose and conjugate transpose, respectively. Finally, the acronym i.i.d. means independent and identically distributed, whereas symbol $E[\cdot]$ denotes statistical expectation.

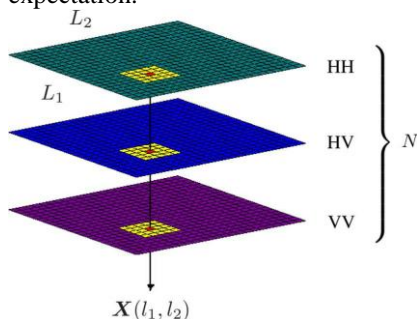


Figure. 1. Pictorial representation of the construction of the data cube for polari-metric images.

III. PROPOSED METHOD

In this paper the manual calculations are overcome by using the SVM classification.. This method detects oil precisely from the other hazardous substances which float on the surface of the oceans. At first the Multipolarized SAR images are taken from the satellite where it is in the RGB format. This image which is being acquired from the satellite is being converted into gray scale where the value ranges from 0-255 where 0 being black and 255 being white. The following represents a Flow chart describing the process.

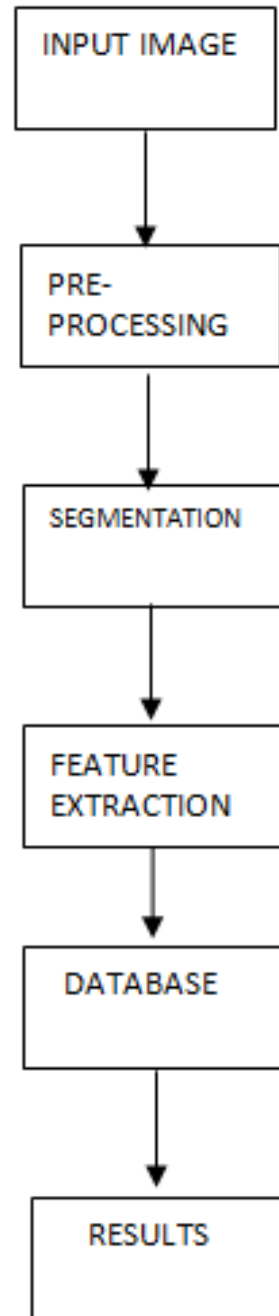


Figure.2. Flow chart Describing the working of the method.

Now the converted gray scale image is filtered to remove the noise and it is being enhanced in order to make the image good for processing. This is done by increasing the contrast from low to high and now the image is obtained. The segmentation

process now involves Thresholding where the default value of threshold is being set for the oil and now each pixel of the image is now being viewed and checked whether there is oil spill or not. This process is now being repeated continuously and the area where the oil is spilled is alone taken and then processed.

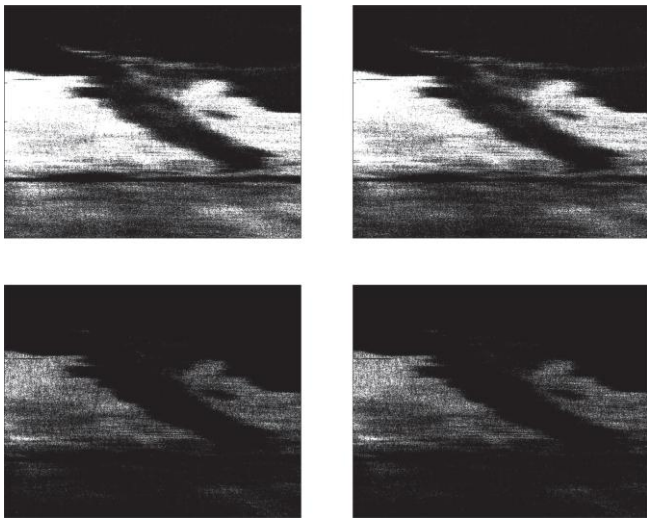


Figure.3. Real SAR L-band data GOMoil_07601_10052_102_100622_L090_CX_02 detection map resulting from the application of a threshold to the span image.

After the segmentation has been completed now the feature extraction process is to be done where the area of oil spill is alone taken and then the area is being calculated. If the area is found to be small then it is being termed as small and if the area is large and then it is taken as large and then it is being stored in the database. Now when the image which is being fed from the satellite is given as input then the following segmentation and feature extraction occurs and the oil spilled area is detected successfully

IV. CONCLUSION:

In proposed method, oil spilling is detected by the segmentation (Thresholding), feature extraction process and classification (SVM). It is free from noise (median filter). In this system, we are detecting the exact oil spilling. It does not undergoes manual calculations.

V. REFERENCES

[1]. "The dumping of hydrocarbons from ships into the seas and oceans of Europe (The other side of oil slicks)," Oceana, Washington, DC, USA, Tech. Rep., Nov. 2003. [Online]. Available: <https://eu.oceana.org/sites/default/files/reports/oilreport-english.pdf>

[2]. G. Franceschetti, A. Iodice, D. Riccio, G. Ruello, and R. Siviero, "SAR raw signal simulation of oil slicks in ocean environments," *IEEE Trans. Geosci. Remote Sens.*, vol. 40, no. 9, pp. 1935–1949, Sep. 2002.

[3] P. Lombardo and C. Oliver, "Optimum detection and segmentation of oil slicks using polarimetric SAR data," *Proc. Inst. Elect. Eng.—Radar, Sonar Navigat.*, vol. 147, no. 6, pp. 309–321, Dec. 2000.

[4] W. Wang, F. Lu, P. Wu, and J. Wang, "Oil spill detection from polarimetric SAR image," in *Proc. IEEE 10th ICSP*, Oct. 2010, pp. 832–835.

[5] R. Shirvany, M. Chabert, and J.-Y. Tournet, "Ship and oil-spill detection using the degree of polarization in linear and hybrid/compact dual-pol SAR," *IEEE J. Sel. Topics Appl. Earth Observ. Remote Sens.*, vol. 5, no. 3, pp. 885–892, Jun. 2012.

[6] J. Fortuny-Guasch, "Improved oil slick detection and classification with polarimetric SAR," in *Proc. POLinsar*, ESA-Esrin, Frascat, Italy, Jan. 2003, pp. 1–5.

[7] M. Migliaccio, A. Gambardella, and M. Tranfaglia, "SAR polarimetry to observe oil spills," *IEEE Trans. Geosci. Remote Sens.*, vol. 45, no. 2, pp. 506–511, Feb. 2007.

[8] P. Lombardo, D. I. Conte, and A. Morelli, "Comparison of optimised processors for the detection and segmentation of oil slicks with polarimetric SAR images," in *Proc. IEEE IGARSS*, 2000, vol. 7, pp. 2963–2965.

[9] Y. Junjun, Y. Jian, Z. Zheng-Shu, and S. Jianshe, "The extended Bragg scattering model-based method for ship and oil-spill observation using compact polarimetric SAR," *IEEE J. Sel. Topics Appl. Earth Observ. Remote Sens.*, vol. 8, no. 8, pp. 3760–3772, Aug. 2015.

[10] L. Yu, Z. Yuanzhi, C. Jie, and Z. Hongsheng, "Improved compact polarimetric SAR quad-pol reconstruction algorithm for oil spill detection," *IEEE Geosci. Remote Sens. Lett.*, vol. 11, no. 6, pp. 1139–1142, Jun. 2014.

[11] A. Solberg, "Remote sensing of ocean oil-spill pollution," *Proc. IEEE*, vol. 100, no. 10, pp. 2931–2945, Oct. 2012.

[12] S. M. Kay, "The multifamily likelihood ratio test for multiple signal model detection," *IEEE Signal Process. Lett.*, vol. 12, no. 5, pp. 369–371, May 2005.

[13] E. L. Lehmann, *Testing Statistical Hypotheses*, 2nd ed. New York, NY, USA: Springer-Verlag, 1986.

[14] R. J. Muirhead, *Aspects of Multivariate Statistical Theory*. New York, NY, USA: Wiley, 1982.

[15] S. V. Nghiem, S. H. Yueh, R. Kwok, and F. K. Li, "Symmetry properties in polarimetric remote sensing," *Radio Sci.*, vol. 27, no. 5, pp. 693–711, Sep./Oct. 1992.

[16] J. S. Lee and E. Pottier, *Polarimetric Radar Imaging: From Basics to Applications*. Boca Raton, FL, USA: CRC Press, 2009.

[17] R. J. Muirhead, *Aspects of Multivariate Statistical Theory*, vol. 197. New York, NY, USA: Wiley, 2009.

[18] S. M. Kay, "Exponentially embedded families—New approaches to model order estimation," *IEEE Trans. Aerosp. Electron. Syst.*, vol. 41, no. 1, pp. 333–345, Jan. 2005.

[19] V. Carotenuto, A. De Maio, C. Clemente, and J. J. Soraghan, "Invariant rules for multipolarization SAR change detection," *IEEE Trans. Geosci. Remote Sens.*, vol. 53, no. 6, pp. 3294–3311, Jun. 2015.

[20] K. Conradsen, A. A. Nielsen, J. Schou, and H. Skriver, "A test statistic in the complex Wishart distribution and its application to change detection in polarimetric SAR data," *IEEE Trans. Geosci. Remote Sens.*, vol. 41, no. 1, pp. 4–19, Jan. 2003.

[21] L.M. Novak, "Change detection for multi-polarization, multi-pass SAR," in *Proc. SPIE Conf. Algorithms Synthetic Aperture Radar Imagery XII*, Orlando, FL, USA, Mar. 2005, pp. 234–246.

[22] L. Mirsky, "On the trace of matrix products," *Mathematische Nachrichten*, vol. 20, pp. 171–174, 1959.

[23] E. J. Kelly, "An adaptive detection algorithm," *IEEE Trans. Aerosp. Electron. Syst.*, vol. 22, no. 2, pp. 115–127, Mar. 1986.